



Differential effects of valley city morphology on mesoscale flow field characteristics



Songheng Wu^{a,b}, Canwen Chen^b, Yi Wang^{a,b,*}, Zhuolei Yu^b, Jiaxuan Cao^b, Ruida Zhang^b, Han Song^c

^a State Key Laboratory of Green Building in Western China, Xi'an University of Architecture and Technology, PR China

^b School of Building Services Science and Engineering, Xi'an University of Architecture and Technology, Xi'an, PR China

^c China Northwest Architecture Design and Research Institute, Xi'an, PR China

ARTICLE INFO

Keywords:
Calm and stable weather
Valley city
Urban form
Mesoscale flow
Numerical water tank

ABSTRACT

The coupling of two mesoscale flows, slope wind and urban heat island circulation (UHIC), is the basic model of valley urban ventilation under calm and stable weather conditions. Under the influence of the economy, history, and landforms, cities may take different forms. However, the different effects of form transformation on the mesoscale flow field characteristics of valley cities under calm and stable weather have not been studied. In this paper, a numerical simulation method, called numerical water tank, is proposed to study the mesoscale flow by using the small-scale method, and then the differential effects of urban expansion and geometric shape transformation on the mesoscale flow field characteristics of valley cities are discussed respectively. This study elucidates the difference in the effects of the valley city form on the mesoscale flow field of valley cities under calm and stable weather conditions. From the perspective of the terrain effect and upslope wind effect, urban expansion is not conducive to the dissipation of heat and pollutants in urban areas. From the aspect of urban geometry, the conditions of atmospheric diffusion are most favorable in the two types of urban layouts: rectangle and square. Downslope wind plays a critical role in improving urban thermal and air environments.

1. Introduction

According to the Statistical Bulletin of the People's Republic of China on National Economic and Social Development 2020, data from the National Bureau of Statistics in 2019 indicate that by the end of 2020, China's urbanization level has exceeded 60% and is in a stage of steady rise. Urbanization causes significant anthropogenic climate change, known as the urban heat island effect [1]. Urbanization may also cause a series of local environmental problems such as weak solar radiation [2–5]: The high concentration of particulate matters in air has greatly reduced the amount of solar radiation that can reach the earth; slow urban wind [6–9]: The high density of tall buildings in cities reduces wind speed in urban areas, which tends to hinder the dissipation of air pollutants and heat, while increasing the energy consumption rate of buildings; haze weather [10–13]: It occurs more frequently in winter and is mainly composed of sulfur dioxide, nitrogen oxides and inhalable particles; and urban warming [14–17]: With the increase of urban area and the passage of time, the temperature of urban area gradually rises.

For cities located in valleys, these local environmental problems will

be even more serious. Because of the different influences of the uneven thermal properties of the underlying surface, the temperature inversion phenomenon known as the "cold pools effect" [18] is more likely to occur in the valley, which has a strong inhibitory effect on air convection. Furthermore, the barrier effect of the terrain can further slow the wind speed of inner cities, eventually leading to worse atmospheric diffusion conditions [19]. Most urban extreme high-temperature events and pollution events occur in the presence of both calm wind and temperature inversion [20,21]. For example, in the Uintah Basin of the United States, the long-term strong temperature inversion causes the pollution released by the oil and gas industry to accumulate and the ozone concentration to significantly exceed the standard [22]. Santiago, the capital of Chile, is one of the cities with the most serious air pollution in the world [23], and according to the data, temperature inversion occurs in Santiago more than 70% of the days each year [24]. When calm wind weather meets relatively stable atmospheric junctions the atmosphere is prone to haze weather [25,26]. At this time, owing to the absence or weakness of large-scale background winds, the ventilation of the valley city can only rely on the slope wind and UHIC formed from natural thermal pressures.

* Corresponding author. State Key Laboratory of Green Building in Western China, Xi'an University of Architecture and Technology, PR China.
E-mail address: wangyi6920@126.com (Y. Wang).

Nomenclature

D	City diameter m
W	Valley floor width m
R	Ratio of valley floor width W to city diameter D
N	Background buoyancy frequency s^{-1}
Fr	Froude number
Ra	Rayleigh number
Nu	Nusselt number
z_{ie}	The simulated mixed height of the city edge m
z_{ic}	The simulated mixed height of the city center m
u_D	Convective velocity scale $mm \cdot s^{-1}$
H_U	Heat fluxes in simulated urban areas $W \cdot m^{-2}$
H_S	Heat fluxes in the simulated slope region $W \cdot m^{-2}$
u	The partial velocity in the z direction $m \cdot s^{-1}$
w	The partial velocity in the x direction $m \cdot s^{-1}$
ρ	Fluid density $kg \cdot m^{-3}$

Under the influence of history, economy, and topography, cities will take different forms [27]. The form here refers not to the compactness of the cities studied by Schneider [28] and Debbage [29], but to the geometric shape of cities, such as “band” and “cluster” [30], which can be specifically reflected in plane geometric structures, such as a rectangle, square, circle, or even a triangle. Real cities don't usually have idealized geometry. However, it is necessary to select idealized geometric shapes in order to realize the comparative analysis of the different effects of different geometric shapes on the flow structure of urban scale from the mechanism level. The aspect ratio of the UHIC is exceptionally small, so that the airflow at the lower level in the proximal source area can interact with the outflow airflow at the upper level. Such an interaction between the inflow and outflow means that the UHIC will be significantly affected by the overall shape of the heat source [31–34]. The observation test conducted by Xu Xiangde et al. [35] demonstrated that a regional convergence or divergence phenomenon appeared in the urban wind field in Beijing, which may be called “diagonal flow.” To the best of our knowledge, no comprehensive and in-depth study has been conducted on the different effects of various urban geometries on the mesoscale flow field characteristics of valley cities. When the width of the valley is small, the expansion of the city is hindered and may appear as a rectangle, while when the width of the valley is large enough, the development of the city is almost unlimited and may appear as a square or circle. This study focuses on rectangular, square, rhombus and circular cities. In addition, with the continuous advancement of urbanization, cities are constantly expanding outward. If a city is in a valley, the ratio of the width of the valley floor to the diameter of the city is shrinking. Studies have determined that the horizontal action range of a plain UHIC usually reaches 2–4 times the city diameter [36–39]. Therefore, if the valley floor width is large enough to prevent the slope and its derived slope winds from influencing the UHIC, then the mesoscale flow field of valley cities is similar to that of plain cities. If the width of the valley floor is small enough and the urban areas cover the valley floor, then the UHIC may not occur due to the “disappearance” of the rural areas, and eventually the diffusion stratification phenomenon similar to the double-diffusion convection study is formed [40]. If the valley floor width is moderate, the slope wind and UHIC can coexist and interact with each other. Hibberd [41,42] demonstrated that in order to avoid the impact on the development of UHIC, the tank used in the water tank experiment should be three times the diameter of the city in design. This also indicates that the mesoscale flow field of the valley city may be affected by the relative size of the valley floor width and the city diameter. No systematic study has been conducted to date. Here, we focus on the cases where the width of the valley floor is 1–4 times the diameter of the city or infinite.

The research methods in this field cover field measurement, theoretical analysis, model experiment and numerical simulation, and each method has its own advantages and applicability, which were reviewed in detail in a previous review article [19]. In particular, water tank experiments and numerical simulations have exhibited substantial benefits and application prospects in the study of mesoscale flows, which deserve extensive attention from researchers. Numerical simulation in this field can be roughly divided into two categories [43]. One is the numerical model which is good at mesoscale simulation, such as weather prediction model (WRF), and the other is the computational fluid dynamics (CFD) method which is good at small-scale simulation. Their biggest advantage lies in saving research cost and shortening research cycle. Savijarvi and Liya [44] used a two-dimensional mesoscale model to analyze the whole-day wind speed in Lanzhou when the wind was calm. The analysis indicates that the wind speed in urban areas is reduced by the coupling effect of the slope wind and UHIC. Huang [45] proposed a two-scale model and used this model to study the influence of the slope angle on the flow structure of UHIC under the terrain effect. They found that even a slight slope would lead to significant changes in the flow structure of UHIC. Ganbat et al. [46] studied the interaction between the slope flow generated by a single mountain and UHIC by combining the WRF model with the University of Seoul's urban canopy model. At present, the simulation of large-scale air flow can be realized by FLUENT. Wang [47] proposed a CFD model based on the coordinate transformation method [48] and successfully implemented it in FLUENT. Using this model, she revealed the effects of different heat fluxes and city heights on UHIC characteristics, but there are still some challenges. Due to the large flow scale, first of all, the anelasticity and compressibility of the atmosphere should be considered. Secondly, the computational resources required may be very large. In view of the water tank experiment, in order to obtain the main characteristics of the UHIC, the scientific problem is simplified to natural convection over isolated horizontal plates of various shapes with a stable stratified background environment (the density or temperature decreases linearly with height). This simplification proved to be reasonable [49], and copper plates with high thermal conductivity were often used as scaled city models. To our knowledge, Shindler and Moroni are the only researchers to study the coupling effect of slope wind and UHIC using water tank experiments. Shindler et al. [50] studied the interaction between the slope wind and UHIC in a narrow valley under static weather conditions using a laboratory model based on a temperature-stratified water tank. Subsequently, Moroni [51] further studied the interaction between the UHIC and upslope wind under unilateral slope conditions on the same water tank experimental platform using feature-tracking technology. However, in the case of symmetric valleys, they focused predominantly on the variations in the heat flux on the slope surface. The most significant advantage of water tank experiment is that it can control the boundary conditions precisely and have high spatial and temporal resolution. In addition, it has many advantages in visualization of flow field, measurement of temperature field and velocity field. However, the water tank experiment also has the problems of high threshold and high cost. Both the preliminary design of the experiment and the “accidents” in the process of the experiment will consume a lot of time and energy of researchers, which makes people eager to find a more efficient research method.

The purpose of this paper is to find a more convenient, efficient and reliable research method for the study of urban scale flow, and to reveal the different effects of urban geometry on the characteristics of valley city mesoscale flow from the mechanism level. In Section 2, the numerical simulation method adopted in this study and the detailed working conditions are described. In Section 3, the numerical simulation results are presented from three aspects: the terrain effect, upslope wind, and downslope wind. In Section 4, the research results are discussed in detail. Relevant research can provide scientific guidance for urban planning and industrial park site selection.

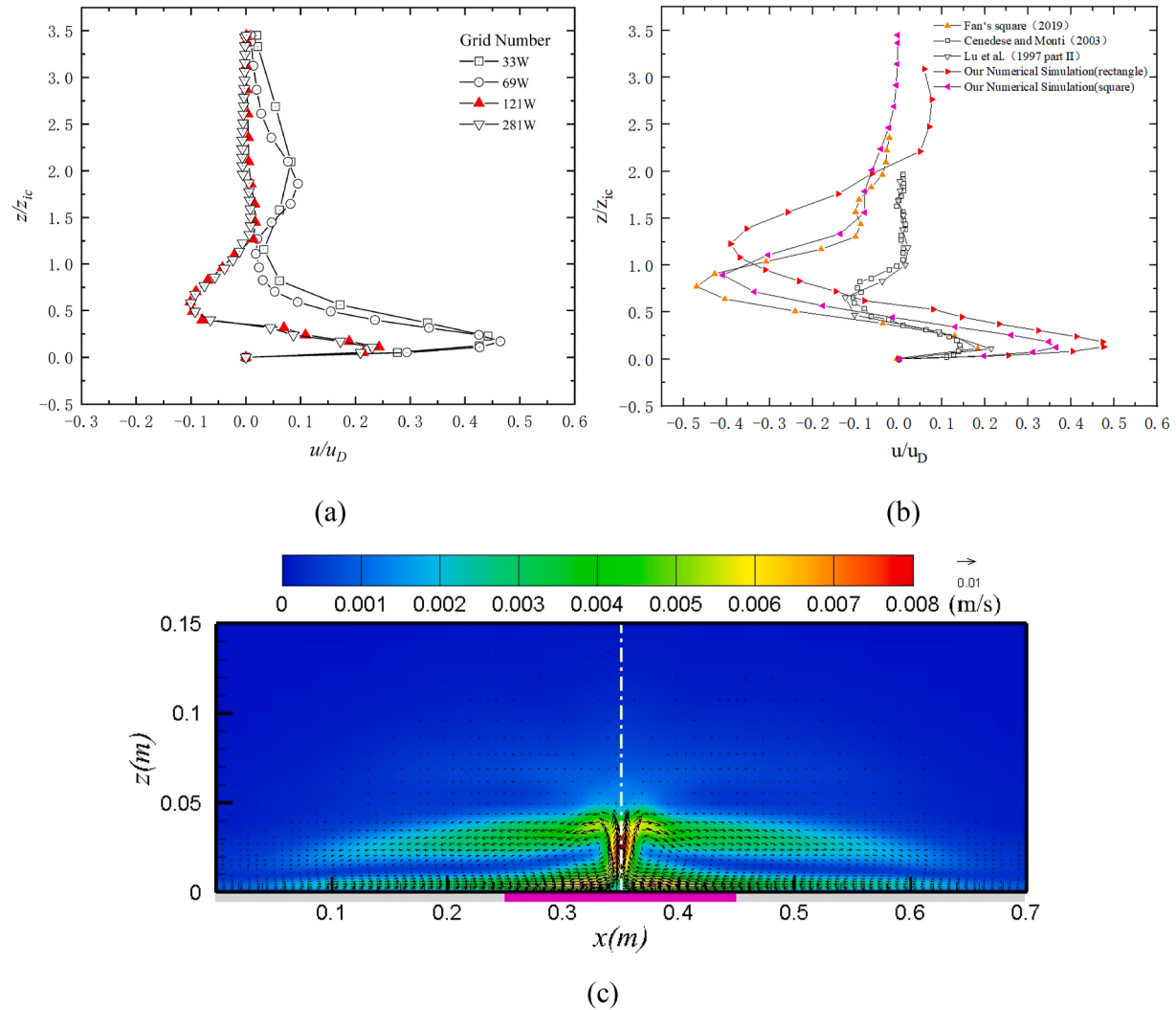


Fig. 1. Verification of numerical simulation model. (a) Vertical dimensionless horizontal velocity distribution of urban edge under different grid numbers; (b) Vertical dimensionless horizontal velocity distribution of urban edge; (c) Velocity fields.

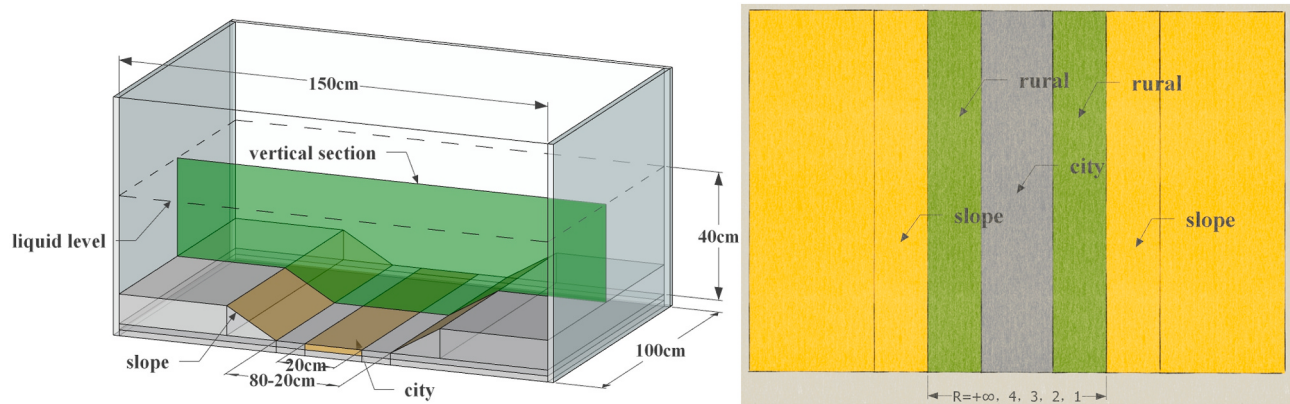


Fig. 2. Schematic diagram of physical model when the valley floor width changes.

2. Methods

As mentioned above, numerical simulation and water tank experiment have their own advantages. At the same time, some scholars have successfully realized the simulation of large-scale air flow with FLUENT, but there are still some challenges. Is there a method that can integrate

the advantages of numerical simulation and water tank experiment, and overcome the disadvantages of FLUENT in large-scale flow simulation?

Fortunately, numerical wind tunnels in the field of wind engineering have given us inspiration, and the application of this method has been very mature [52], and many valuable research results have been obtained. On this basis, the idea of direct simulation of water tank

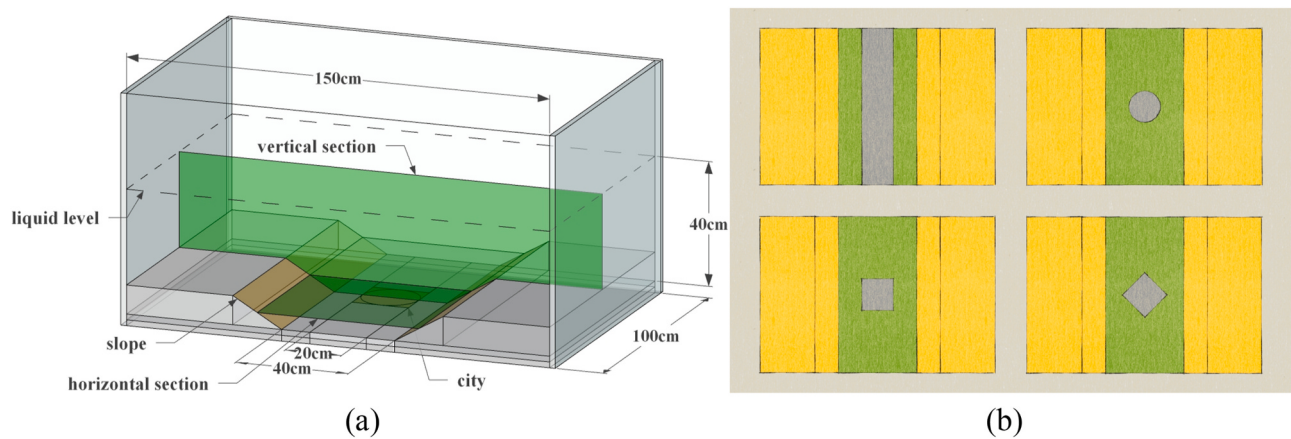


Fig. 3. (a) Schematic diagram of the physical model (changes in the urban geometrical morphology); (b) Urban form diagram (from left to right and from top to bottom, rectangular, round, square, and rhombus).

Table 1

Working conditions; the variable is the ratio of valley floor width W to the city diameter D ($R = \infty, 4, 3, 2, 1$).

Case	The bottom width (W)	Urban heat flux (H_U) $\text{W}\cdot\text{m}^{-2}$	Slope heat flux (H_S) $\text{W}\cdot\text{m}^{-2}$	Convective velocity scale (u_D) $\text{mm}\cdot\text{s}^{-1}$	Background buoyancy frequency (N) s^{-1}	City diameter (D) m	Froude number (Fr)
1	$+\infty$	5500	\	8.76	1	0.2	0.044
2	4D	5500	0	8.76	1	0.2	0.044
3	3D	5500	0	8.76	1	0.2	0.044
4	2D	5500	0	8.76	1	0.2	0.044
5	1D	5500	0	8.76	1	0.2	0.044
6	4D	5500	2750	8.76	1	0.2	0.044
7	3D	5500	2750	8.76	1	0.2	0.044
8	2D	5500	2750	8.76	1	0.2	0.044
9	1D	5500	2750	8.76	1	0.2	0.044
10	4D	5500	-2750	8.76	1	0.2	0.044
11	3D	5500	-2750	8.76	1	0.2	0.044
12	2D	5500	-2750	8.76	1	0.2	0.044
13	1D	5500	-2750	8.76	1	0.2	0.044

Table 2

Working conditions; the variable is urban geometry (rectangle, square, rhombus, circle).

Case	The bottom width (W)	Urban heat flux (H_U) $\text{W}\cdot\text{m}^{-2}$	Slope heat flux (H_S) $\text{W}\cdot\text{m}^{-2}$	Convective velocity scale (u_D) $\text{mm}\cdot\text{s}^{-1}$	Background buoyancy frequency (N) s^{-1}	urban geometry	City diameter (D) m	Froude number (Fr)
1	2D	5500	0	8.76	1	rectangle	0.2	0.044
2	2D	5500	0	8.76	1	square	0.2	0.044
3	2D	5500	0	8.76	1	rhombus	0.2	0.044
4	2D	5500	0	8.76	1	circle	0.2	0.044
5	2D	5500	2750	8.76	1	rectangle	0.2	0.044
6	2D	5500	2750	8.76	1	square	0.2	0.044
7	2D	5500	2750	8.76	1	rhombus	0.2	0.044
8	2D	5500	2750	8.76	1	circle	0.2	0.044
9	2D	5500	-2750	8.76	1	rectangle	0.2	0.044
10	2D	5500	-2750	8.76	1	square	0.2	0.044
11	2D	5500	-2750	8.76	1	rhombus	0.2	0.044
12	2D	5500	-2750	8.76	1	circle	0.2	0.044

experiment is proposed.

It is undeniable that the water tank experiment is a model experiment after simplified assumptions, and the dimensionless number between the model flow and the prototype flow cannot be equalized one by one [53], which will inevitably bring some errors. If on this basis, using numerical simulation method to simulate the water tank experiment instead of the real atmosphere flow will introduce quadratic error. However, this paper intends to make a beneficial attempt to solve large-scale problems using small-scale methods, which is called “numerical water tank” here. As the physical process is clear, the geometric

scale after scaling is small, and can be directly compared with the experimental data of the water tank, this method will greatly improve the computational efficiency, save the research cost, and provide a new idea for the study of mesoscale flow.

2.1. Basic equations

The mesoscale flow in valley cities is subordinate to the atmospheric boundary layer flow. The equation of motion reflects the dynamic relationship of the atmospheric boundary layer. But it is not enough,

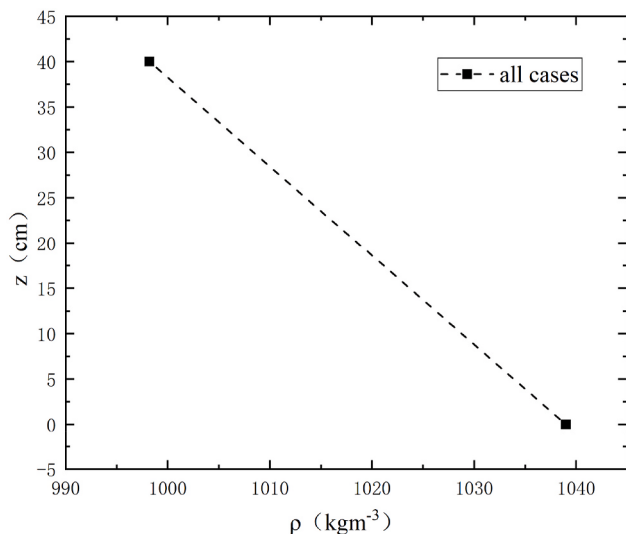


Fig. 4. Density profiles corresponding to all cases.

because in the process of motion, the state parameters of air are changing all the time, so it is necessary to supplement the continuity equation, thermodynamic equation and equation of state. Assuming that the air is an incompressible ideal gas, the equation of state can be omitted. Since wet air is not considered here, there is no need to increase the water vapor equation. In addition, when the object of study is no longer the small scale, the Coriolis effect, which refers to the motion of air micromasses relative to the earth due to the rotation of the earth, should be considered in the model experiment, but this part of the force is further ignored in the numerical simulation. Because the atmospheric boundary layer is a shallow fluid and the velocity of motion is much less than the speed of sound, the Boussinesq approximation can be applied in the atmospheric boundary layer, which means that in the buoyant flow problem with little change in density, the change of density is only considered in the gravity term of the governing equation, but not in other terms. In this way, the basic equations of the atmospheric boundary layer can be simplified as follows:

1. Continuity equation

$$\frac{\partial u_i}{\partial x_i} = 0 \quad (1)$$

2. Equation of motion

$$\frac{\partial u_i}{\partial t} + u_j \frac{\partial u_i}{\partial x_j} = -\frac{1}{\rho} \frac{\partial p}{\partial x_i} + v \frac{\partial^2 u_i}{\partial x_j \partial x_j} + g \frac{\theta}{T} \delta_{3i} \quad (2)$$

3. Thermodynamic equation

$$\frac{\partial \theta}{\partial t} + u_j \frac{\partial \theta}{\partial x_j} = k_T \frac{\partial^2 \theta}{\partial x_i \partial x_i} \quad (3)$$

The Einstein summation convention is used here, that is, if there is a duplicate subscript in an item, it means that the subscript should be summed. The fluid unsteady acceleration plus convective acceleration on the left side of equation (2.2) is equal to the sum of the pressure gradient force, molecular viscous force and buoyancy on the right. Where:

v is the moving viscosity coefficient of air;

δ_{ij} is a Kronecker function, when $i = j$, $\delta_{ij} = 1$; otherwise, $\delta_{ij} = 0$; Equation (2.3) is a heat transport equation. After ignoring latent heat

and net radiation, only molecular heat conduction is left as the source term for potential temperature change. Where:

k_T is the thermal conductivity of air, $k_T = \frac{K_T}{\rho C_p}$. Where K_T is the molecular thermal conductivity; θ is the atmospheric potential temperature, and K refers to the temperature at which the atmosphere expands or compresses to the standard pressure from the original pressure and temperature.

2.2. Grid independence and model validation

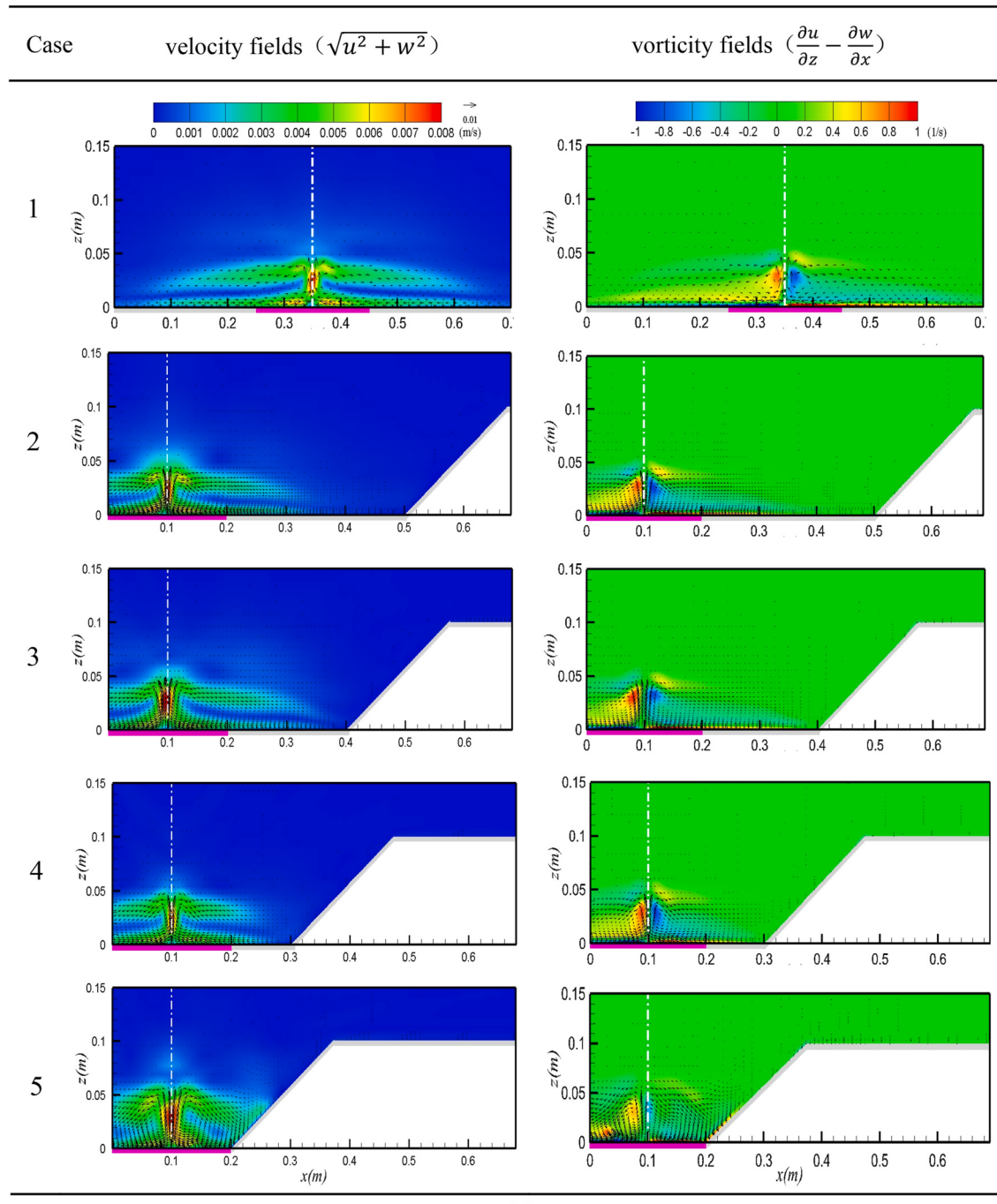
We performed the following numerical simulations on FLUENT2020R1. The numerical simulation physical model of this study was established according to the ideal normal form of a valley city-scale model. The calculated domain length \times width \times height = 1.5 m \times 1.0 m \times 0.4 m. In this study, the fluid medium was set as water with different densities, the ambient temperature was set as 298 K, the heating and cooling of cities and slopes was controlled by a second type of boundary condition (heat flux), and all the other wall surfaces were set as adiabatic non-slip walls. In the numerical simulation process, a density stratified layer is required to simulate the inversion layer. To achieve density stratification, we defined two different water densities (equivalent to brine), and then, with the help of the user-defined function, mixed the two in a certain proportion as the height changed, obtaining the linear density stratification. The research focused on the flow near the wall, so the near-wall model approach was adopted. The SST $K-\omega$ model was selected as the turbulence model to manage the effects of turbulence pulsation and near-wall viscosity.

Four sets of structured grids were selected for the grid number independence test, and the number of grids was 3.3×10^5 , 6.9×10^5 , 1.21×10^6 , and 2.81×10^6 , as displayed in Fig. 1. When the number of grids reached 1.21×10^6 , the change in the wind speed profile on the left edge of the city was exceptionally close, so it can be considered that the number of grids no longer impacted the calculation results at this time. Therefore, considering the calculation speed and accuracy, all the numerical simulation calculations in this study adopted the mesh division method when the mesh number was 1.21×10^6 .

Since it is difficult to obtain the flow field data of valley cities from the literature, this study selects the water tank experiment data of plain cities to compare and verify our numerical simulation results of plain cities. If the verification results are reasonable, it can be inferred that the numerical simulation data of valley cities with the same setting is also credible. In comparison, in both the experimental and numerical simulations, the corresponding initial boundary conditions were consistent, with the city diameter $D = 0.2$ m, heat flux $Q = 5500 \text{ W m}^{-2}$, and density stratification $d\rho/dz = -101.84 \text{ kg m}^{-4}$ (corresponding to background buoyancy frequency $N = 1 \text{ S}^{-1}$ and $Fr = 0.0438$, meeting the similarity requirement [54]), and the ambient temperature is set at 298 K.

Mixing height, which is defined as the height corresponding to the maximum negative buoyancy, is often used in flow field analysis [54]. In practice, a height corresponding to a vertical velocity less than the critical value (10^{-4} m s^{-1}) is usually selected [49]. It should be noted that the mixing height is not a fixed value and varies depending on the location chosen. For example, the mixing height (z_{ie}) of the city edge is approximately 2/3 of the mixing height (z_{ic}) of the city center [32,55]. Usually, the thermal environment in the water tank enters a quasi-steady state 10 min after the heating starts [33]. In this study, the data from 15 min after the heating began was uniformly selected as the effective data for analysis.

The numerical simulation data verified by grid independence were compared with the water tank experiment data of previous research [49, 54, 56]. These studies use water tanks as research methods, where water is used instead of air, and copper heaters are used to simulate cities. They all focus on UHIC under calm and stable weather. Fan [49] used water tank experiments to study the average recirculation flow and turbulent plume structure. Lu [54] discussed the effects of mixing height,



(a)

Fig. 5. Under the action of the terrain effect (case 1–5, valley floor width decreases continuously) (a) velocity fields and vorticity fields; (b) Relationship between Fr and the aspect ratio of the urban thermal plume; (c) Vertical dimensionless horizontal velocity distribution at urban edges; (d) The relation between Ra and Nu .

heat island intensity on urban surface heating rate, heat island size and environmental temperature gradient through water tank experiment. Cenedese [56] used water tank experiments to study the interaction between inland urban heat islands and ocean currents.”

The evaluation was made from two aspects of the flow pattern and the wind speed profile at the urban edge. It can be observed in Fig. 1(c) that the numerical simulation can reproduce the flow phenomenon observed in the experiment well; that is, the characteristics of the UHIC are convergence inflow at the lower level, upward flow over the center (mainly vertical component), and divergence outflow at the upper level. It can be observed in Fig. 1(b) that the wind speed profile on the left edge

of the city is in good agreement with the previous experimental data [49, 54, 56], and the average error between it and Fan's water tank experiment was 13.08% (rectangle) and 2.64% (square). The maximum deviations are 171.16% (rectangular) and 123.18% (square) in the convergent flow zone of the lower layer. This may be caused by the failure to consider the surface roughness of the model in the numerical simulation. In addition, although copper is a good heat conductor, the experimental process cannot guarantee a uniform heat flux on the heating plate surface.

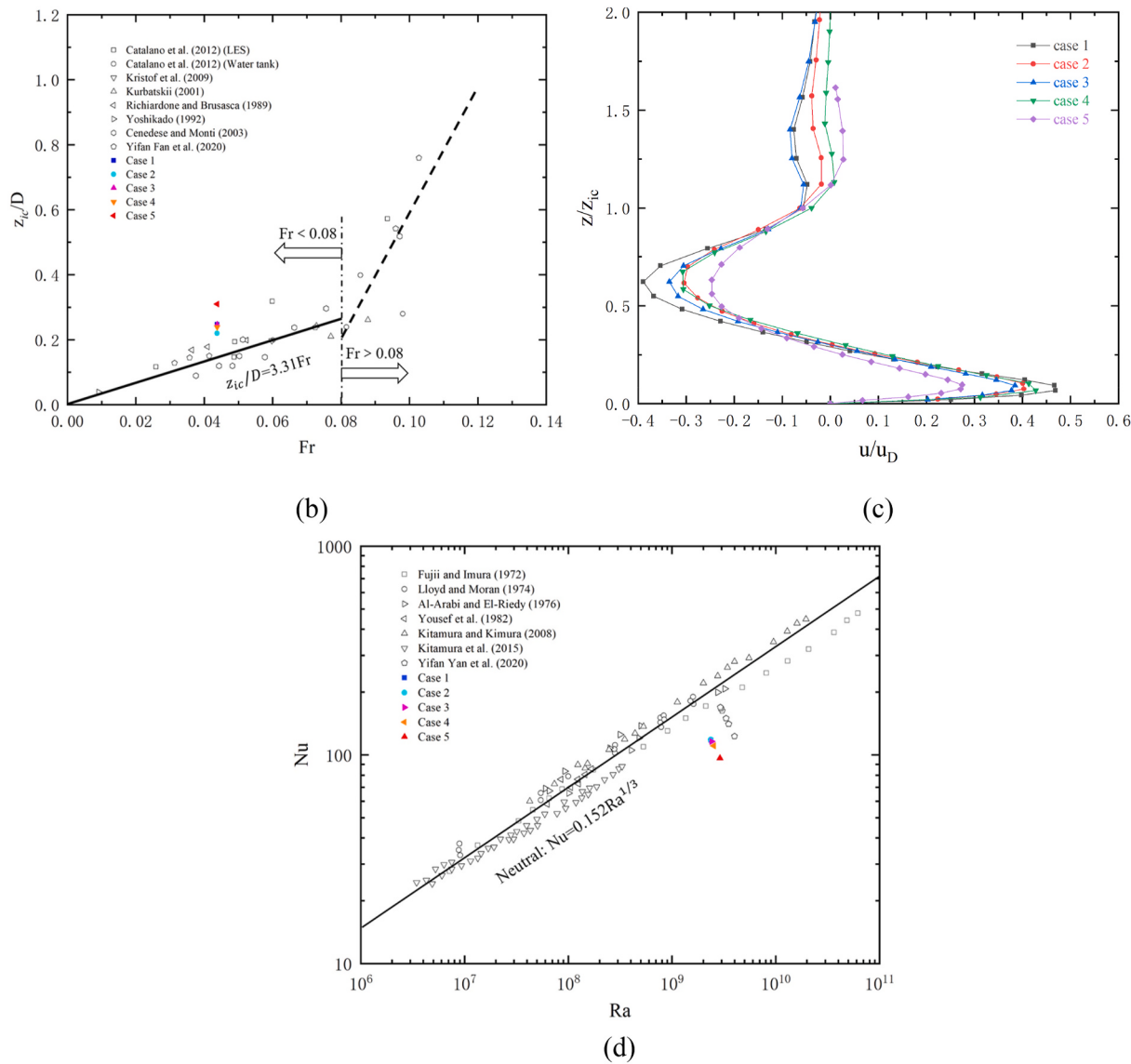


Fig. 5. (continued).

2.3. Numerical simulation setup

This paper does not directly consider meteorological parameters and urban parameters, but indirectly considers the effects of these influencing factors, and also takes background stratification intensity and urban surface heat flux as the control variables in this paper. As for the scalability and compactness of a city, we believe that to some extent, it still affects the urban surface heat flux. Compared with this, this paper is more concerned about the differential influence of urban geometry on the mesoscale flow characteristics.

In Section 3.1, R , the ratio between the valley floor width and city diameter, was selected as the independent controlling variable to discuss the influence on urban expansion on the mesoscale flow field characteristics of the valley cities. The physical model is illustrated in Fig. 2. The thickness of the inversion layer was uniformly set at 40 cm, and the vertical section was the central section of the flow field selected for the analysis.

This section focuses on five situations in which the ratio of the valley floor width to the city diameter ($W/D = R$) is ∞ , 4, 3, 2, and 1, as shown in Fig. 3. Similarly, the terrain effect, upslope wind, and downslope wind are discussed. The corresponding working conditions are presented in Table 1. The heat flux in the urban area under all working conditions

was set as $H_u = 5500 \text{ W m}^{-2}$, without considering heat loss.

In Section 3.2, the geometric forms of cities are selected as the independent controlling variable to discuss the influence on the mesoscale flow field characteristics of valley cities. The physical model is shown in Fig. 3(a). The liquid level height was uniformly set at 40 cm. To investigate the influence of urban geometric morphology transformation, the vertical section of the flow field and the horizontal section at a certain height were selected simultaneously.

This section focuses on four situations: rectangle, circle, square, and rhombus, as shown in Fig. 3(b). The corresponding working conditions are presented in Table 2. The heat flux in urban areas under all working conditions was set as $H_u = 5500 \text{ W m}^{-2}$, without considering heat loss.

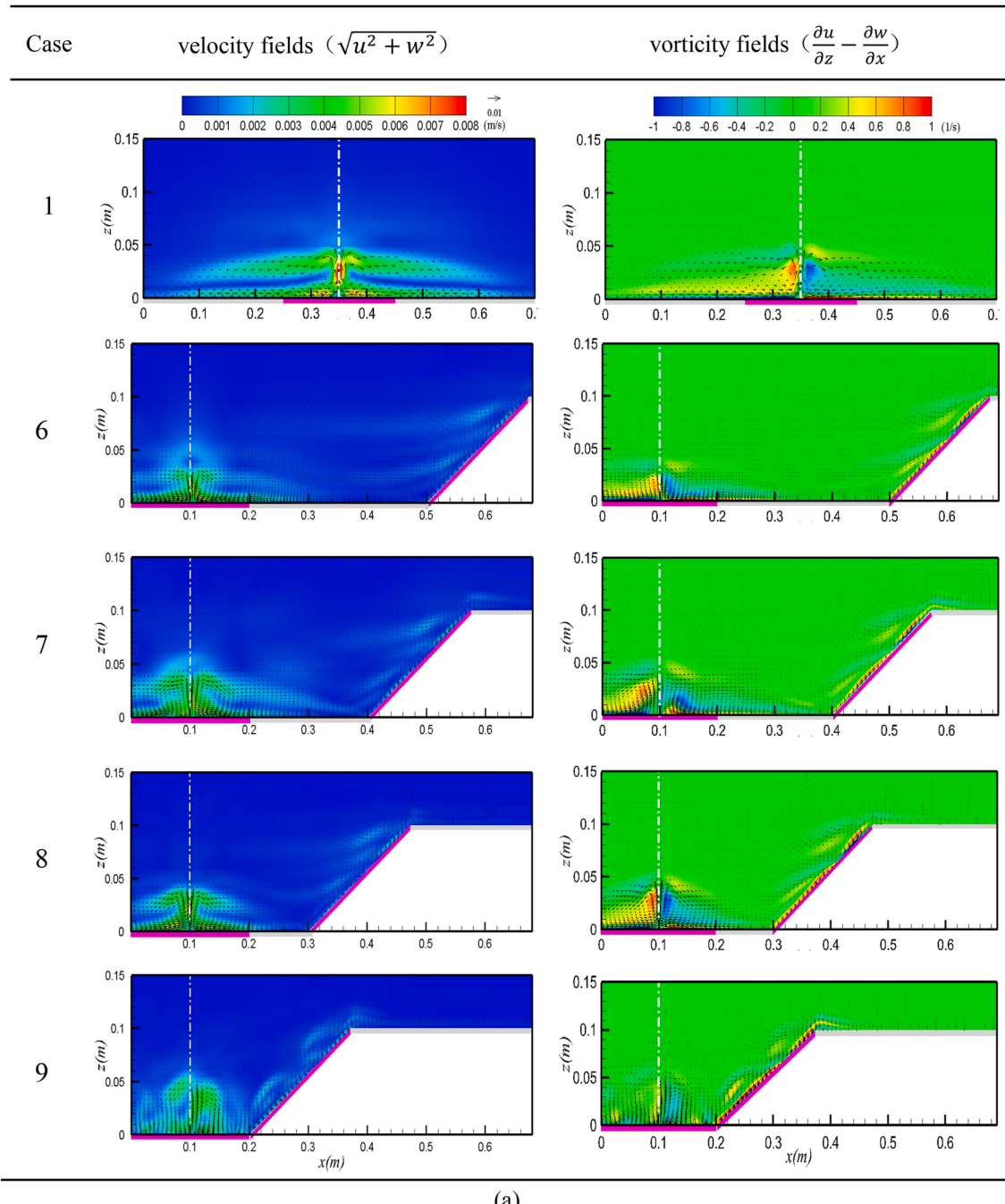
All the above cases adopt the same density stratification intensity of $-101.94 \text{ kg m}^{-4}$, as shown in Fig. 4, and the corresponding Fr is 0.044, which meets the similarity requirements discussed by Lu et al. [54].

3. Results

3.1. Effects of urban sprawl on mesoscale flow field characteristics

3.1.1. The terrain effect

As shown in Fig. 5(a), the velocity and vorticity fields of urban



(a)

Fig. 6. Under the action of upslope wind (case 1, 6–9, the width of valley floor decreases continuously) (a) velocity fields and vorticity fields; (b) Relationship between Fr and aspect ratio of urban thermal plume; (c) Vertical dimensionless horizontal velocity distribution at urban edges; (d) The relation between Ra and Nu .

expansion conditions under the influence of the simple terrain effect are presented. In all the cases, the UHIC structure features convergent inflow in the lower layer, upward flow over the city center, and divergent outflow in the upper layer. The level range of UHIC in plain cities is approximately three times the city diameter. With a decrease in the ratio R between the valley floor width and the city diameter, the horizontal development of the UHIC is gradually restricted by the valleys on both sides, and the corresponding mixing height is continuously increasing. Furthermore, it can be seen from the vorticity fields that the shear zone tends to elongate from the horizontal direction to the vertical direction.

As shown in Fig. 5(b), for the pure terrain effect, the smaller R is, the larger the corresponding mixing height will be. Furthermore, the

convergence and divergence rates of the UHIC are weakened, which means that urban expansion is detrimental to the ventilation of the valley city, and this effect is most significant when the city fills the bottom of a valley. This is probably because urban expansion means shrinking rural areas, making it more difficult for UHIC to develop. Under the simple terrain effect, with a decrease in R , the heat transfer coefficient of the urban canopy surface gradually decreases, which will lead to the deterioration of the urban thermal environment. This may be because when the valley floor is narrower, the corresponding convection velocity is weaker, which has an adverse effect on the heat transfer of the urban canopy surface.

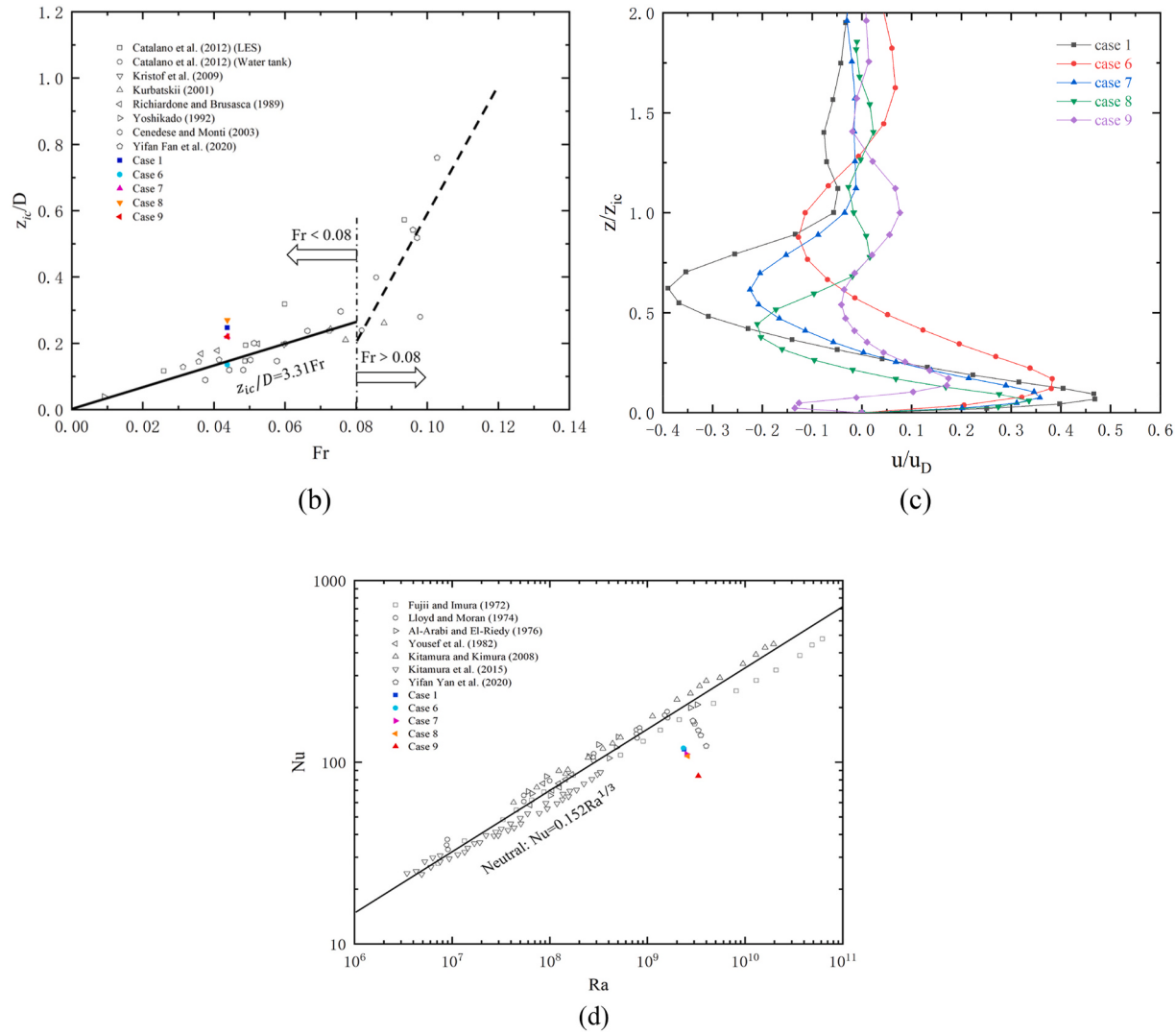


Fig. 6. (continued).

3.1.2. The upslope wind effect

As shown in Fig. 6(a), the velocity and vorticity fields of urban expansion under the action of upslope winds are given. Because it is difficult to form a strong upslope wind when $N = 1.0 \text{ s}^{-1}$, no significant interaction between the upslope wind and UHIC is observed in the image. When $R > 1$, the divergence of the upper layer of the UHIC and the upslope wind form a weak “chain flow” effect. In particular, when $R = 1$, the circulation disappears because the UHIC is essentially caused by the temperature difference between the city and the surrounding countryside area or environment, while the rural area has disappeared; additionally, the temperature of the slopes (heat flux) is substantial, and there is no effective temperature difference.

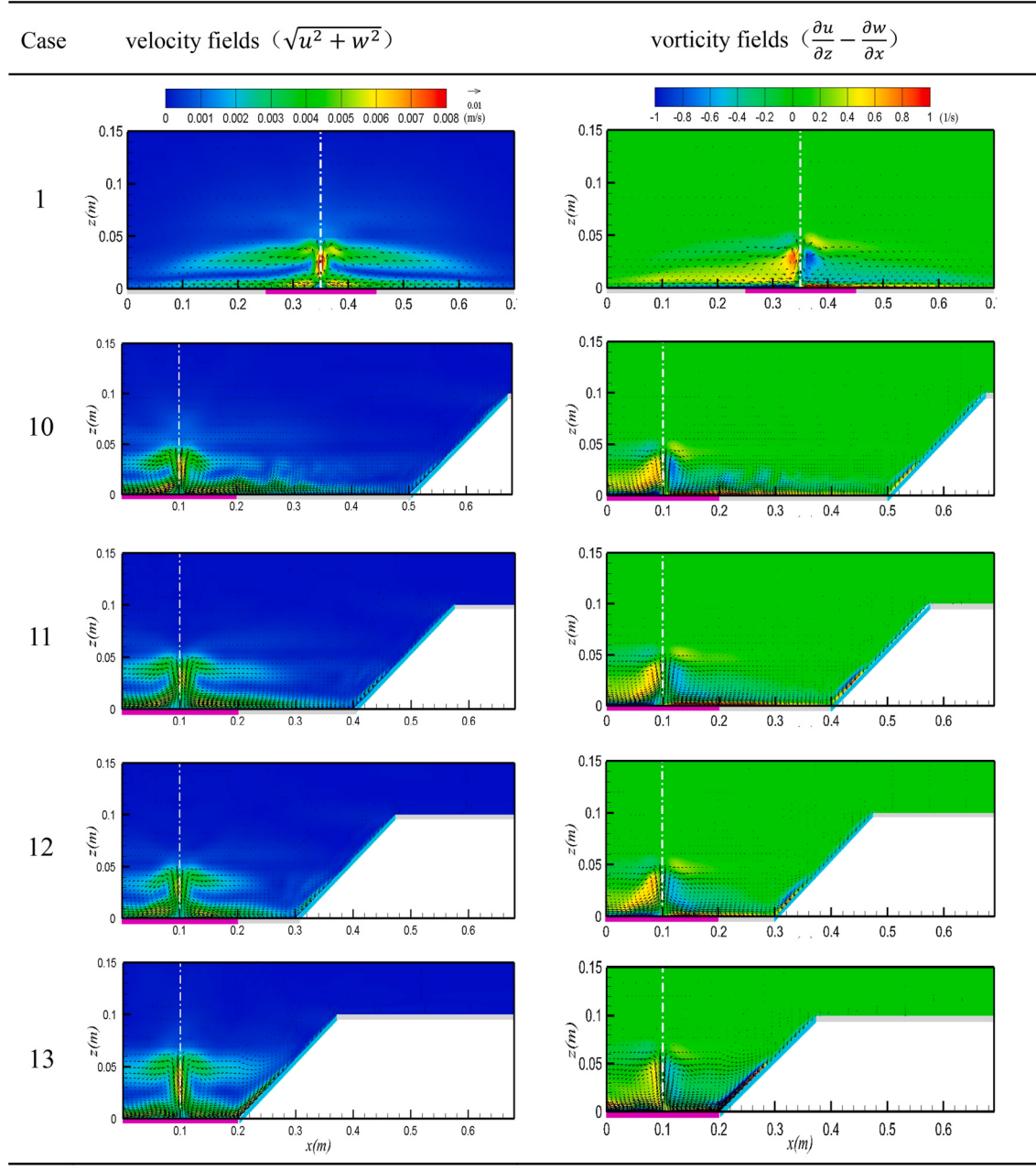
As shown in Fig. 6(b), the mixing height of the urban center under the action of the upslope wind does not change significantly with R , possibly because under the influence of upslope wind, it is no longer appropriate to continue to select the height corresponding to the vertical velocity less than the critical value (10^{-4} m s^{-1}) as the mixing height. At this time, owing to the competition between the upslope wind and UHIC in the lower layer, the development of the UHIC was weakened, and a stagnant zone was formed. As the width of the valley floor decreases, this competition becomes more intense, and eventually, there is no regular circulation in the valley. However, it can be seen from the maximum values of convergence and divergence of UHIC that they will decrease with a decrease in R , which will lead to a decline in the

ventilation capacity in urban areas. Under the effect of the upslope wind, the trend of the heat transfer coefficient of the urban canopy surface is similar to that under the influence of the simple terrain effect, and the reason is the same.

3.1.3. The downslope wind effect

As shown in Fig. 7(a), contrary to the upslope wind, the downslope wind plays a significant role in promoting the development of UHIC. Even when the width of the valley floor is four times the city diameter, the cool and clean downslope wind can flow to the city center through the convergence of the lower level of the UHIC, which is conducive to improving the thermal environment and air quality of the urban area. With the decrease in the width of the valley floor, the promoting effect becomes stronger, and the mixed height of the urban center increases overall. In particular, it can be seen from case 13 that although the rural areas disappeared, UHIC eventually formed under the action of the downslope wind. This is because there is a temperature difference between the urban areas and slopes. In other words, the existence of rural areas is not a necessary condition for the formation of circulation, but a temperature difference is required.

As shown in Fig. 7(b), with the decrease in R under the action of the downslope wind, the mixing height of the urban center presents a trend of gradual increase overall, which still reflects the promotion effect of the valley addition on the longitudinal development of the UHIC. As



(a)

Fig. 7. Under the action of downslope wind (case 1, 10–13, the width of valley floor decreases continuously) (a) velocity fields and vorticity fields; (b) Relationship between Fr and aspect ratio of urban thermal plume; (c) Vertical dimensionless horizontal velocity distribution at urban edges; (d) The relation between Ra and Nu .

shown in Section 3.1.1, under the simple terrain effect, with a decrease in R , the convergence and divergence velocities of the UHIC are both weakened; however, under the action of the downslope wind, such a rule is no longer established, as shown in Fig. 7(c). This may be because the downslope wind is not strictly steady in the process of flowing to the urban area, and the distance from the slope to the urban is not equal. Finally, the downslope current received by the UHIC is partially random, and it is inevitable that the downslope wind does not follow the original flow pattern. The downslope wind significantly promotes the improvement in the urban canopy surface heat transfer coefficient, which is enhanced with a decrease in the valley floor width. The heat transfer coefficients of cases 11 and 12 were equal to those of the neutral environment, and case 13 was even better than that of the neutral environment. To effectively utilize the downslope wind to ventilate the city,

the diameter of the city should be greater than 1/3 of the valley floor width ($R = 3$).

3.2. Effects of urban geometry on mesoscale flow field characteristics

3.2.1. The terrain effect

As shown in Fig. 8, the UHIC structure is similar to that of Fan et al. [33]. However, a weak flow area appeared when Fan studied a rectangular city (length to width ratio 4:1), but it did not appear here. This is because the end of the rectangular city in this study is connected to the wall surface, and the uniform heat flux can be easily realized on the city surface using a numerical simulation, so the flow field finally obtained is similar to two-dimensional flow, which is difficult to achieve experimentally. In addition, obvious diagonal flows can be observed in the

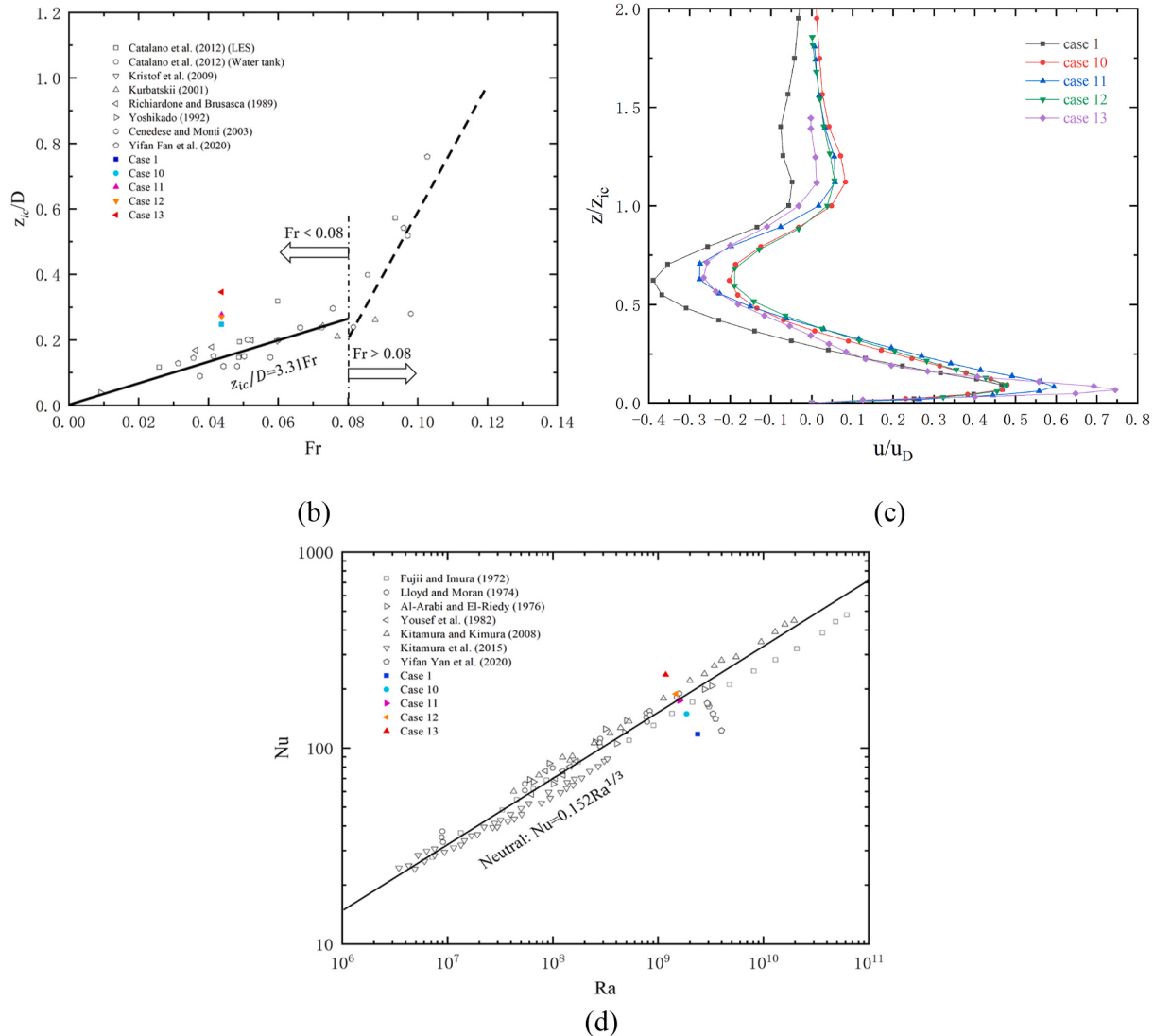


Fig. 7. (continued).

velocity fields of the square and rhomboid urban layouts. Building industrial park sites should be avoided in this area to prevent pollutants from being transported to the city center by strong convergence currents. Here, the horizontal development of the UHIC is restricted by the valleys on both sides, and the flow tends to develop along the valley axis.

As shown in Fig. 9, under the terrain effect, the rectangular city center had the highest mixing height, while the rhombus had the lowest. This indicates that, with all other things being equal, a city in a valley should be designed as a rectangle for greater environmental capacity. At this point, the convergence of the rectangular city is the strongest, and the divergence of the square city is the strongest (because the convergence of the square city is along the diagonal, and the divergence is perpendicular to the length of the side), and for the case of rhombus, both the convergence and divergence are the least. The change in the urban shape under the terrain effect has a different influence on the heat transfer coefficient of its canopy surface, but this difference is not significant. This could be further studied in the future.

3.2.2. The upslope wind effect

As shown in Fig. 10, there was no strong upslope wind at $N = 1.0 \text{ s}^{-1}$, so the flow pattern characteristics of the UHIC observed here were almost the same as those observed under the simple terrain effect. In particular, the “chain flow” phenomenon is formed between the UHIC

outflow and upslope wind.

Similarly, as shown in Fig. 11, under the action of the upslope wind, the rectangular city still has the highest mixing height and the largest corresponding environmental capacity. At this time, the maximum velocity of convergence and divergence of the UHIC is weakened. This indicates that the addition of upslope wind slows down the wind speed in urban areas. In contrast, the rectangular and square layouts were still the best. The change in urban geometry under the effect of upslope wind changes the heat transfer coefficient of the urban canopy surface, but the difference between them is still not significant.

3.2.3. The downslope wind effect

As shown in Fig. 12, the downslope wind greatly promoted the development of the UHIC, and the velocity of low-level convergence under various urban layouts was improved, with rectangular cities being the most prominent. Because downslope winds usually carry cool, clean air, they help dissipate heat and pollutants from urban areas. The UHIC in various geometric forms is “squeezed” by the downslope wind. For square, rhomboid, and even circular urban layouts, the UHIC has a substantial divergent outflow in the direction of the valley axis. Under different urban layouts, when the UHIC is coupled with the slope wind, a convergence flow zone with a range far larger than the city diameter will appear, which will affect the planning and site selection of industrial

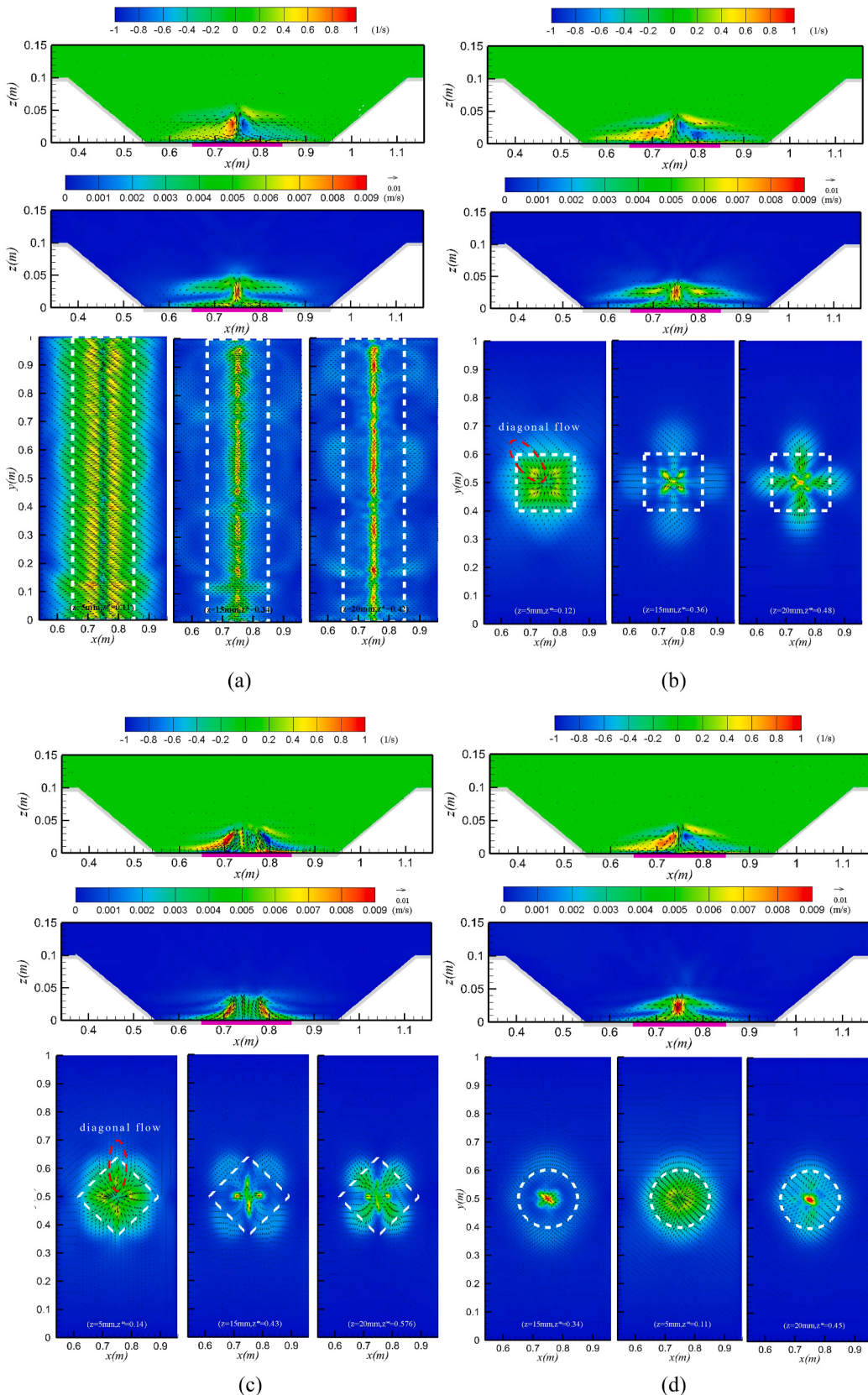


Fig. 8. Velocity fields and vorticity fields under the terrain effect (a, b, c, and d correspond to cases 1, 2, 3, and 4, which are rectangle, square, rhombus, and circle, respectively).

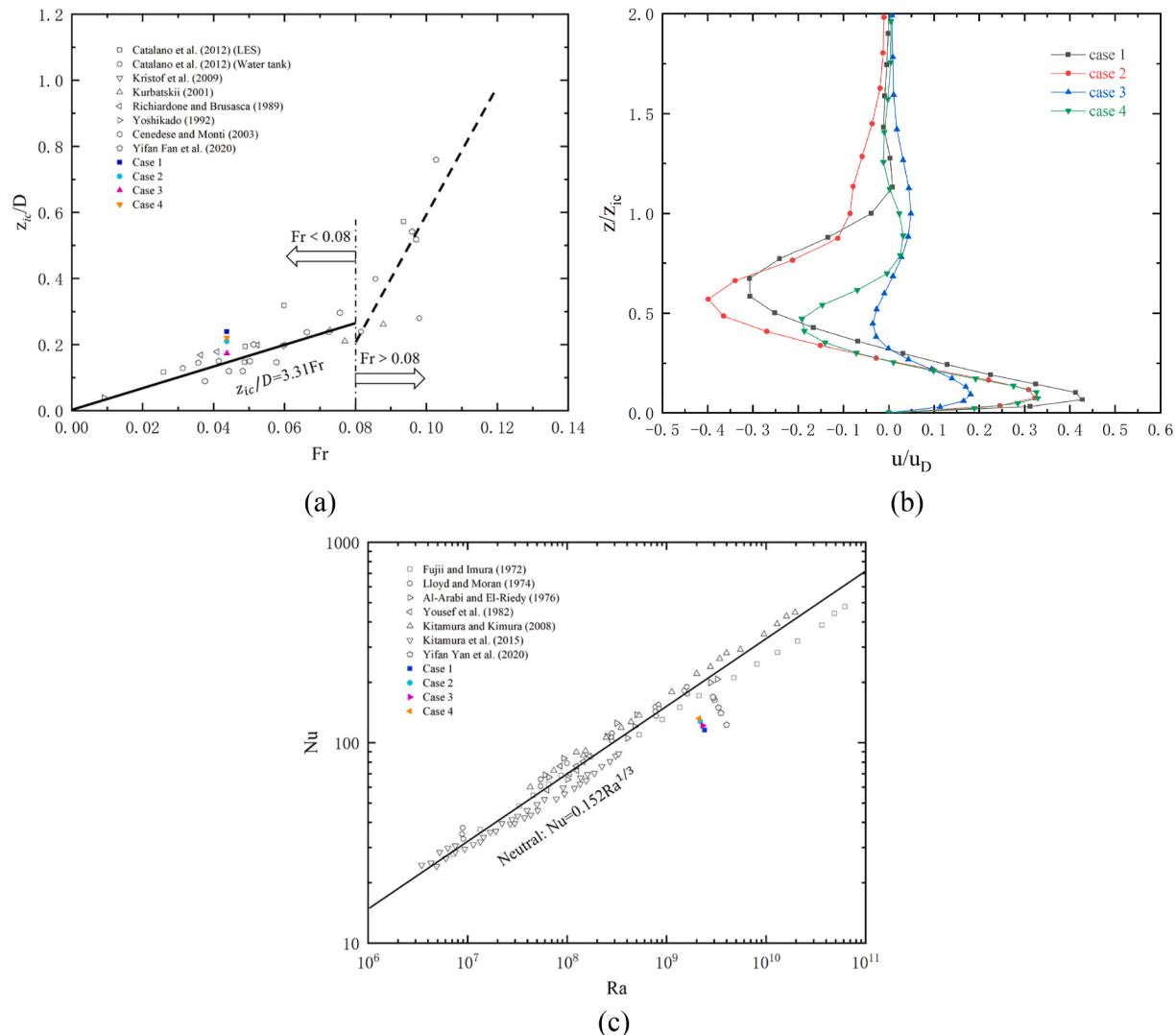


Fig. 9. Under the terrain effect (cases 1, 2, 3, and 4, which are rectangle, square, rhombus, and circle, respectively); (a) Relationship between Fr and aspect ratio of urban thermal plume; (b) Vertical dimensionless horizontal velocity distribution at urban edges; (c) The relation between Ra and Nu .

parks. For a rectangular urban layout, because the flow field is similar to a two-dimensional flow, an industrial park can be planned at both ends of the valley axis. For other urban layouts, owing to the existence of a weak flow zone near the valley axis and the range of the convergence flow zone can reach more than three times the city diameter, the industrial park at this time should be planned near the valley axis and far from the range of three times the city diameter.

As shown in Fig. 13, under the action of the downslope wind, the mixing height of the urban center will also change with the transformation of the geometric form, in which the rectangular city still performs best. In view of the maximum velocity of divergence and convergence of the UHIC, the rectangular and square urban layouts still perform the best. The above phenomenon again suggests that a city designers in the valley should first choose the rectangular layout, then the square layout, and try not to choose the rhombus layout. The surface heat transfer coefficients of the urban canopy under all geometrical forms under the downslope wind were close to a neutral environment. This demonstrates that the downslope wind is helpful in alleviating the urban heat island effect.

4. Discussion

The contribution of this study is to examine the mesoscale flow field

characteristics under different valley urban forms, which include the relative size of the valley floor width and city diameter and the shape of the city itself, in order to provide scientific guidance for urban planning and industrial park site selection. The plain city level of the UHIC is usually 2 to 4 times the diameter of the city [36]. However, the UHIC in valley cities is restricted by valleys on both sides, and its diameter varies with the ratio of the width to the city diameter ($W/D = R$). When $R = 4$, the valley level of the UHIC scope may reach approximately twice the diameter of the city, and when the urban expansion spreads over the valley floor, the heat island circulation is difficult to form under the terrain effect and upslope wind, which is consistent with the conclusion of Bao [40]. However, the UHIC can still be maintained under a downslope wind, which proves that the temperature difference is the fundamental factor for the formation of the UHIC. The results of the study on the shape of cities are basically consistent with Fan's previous studies on plain cities, that is, low horizontal diagonal inflow and high horizontal vertical urban edge diverges the outflow, and the inflow increases in urban areas. In addition, regardless of the effect of slope flow or simple topographic effect, the mixed height of the rectangular and square cities in all four shapes is higher, which means that the environmental capacity is larger under the same conditions. In general, the flow tends to develop along the valley axis because of the restriction of the valleys on either side. Furthermore, the downslope wind promotes

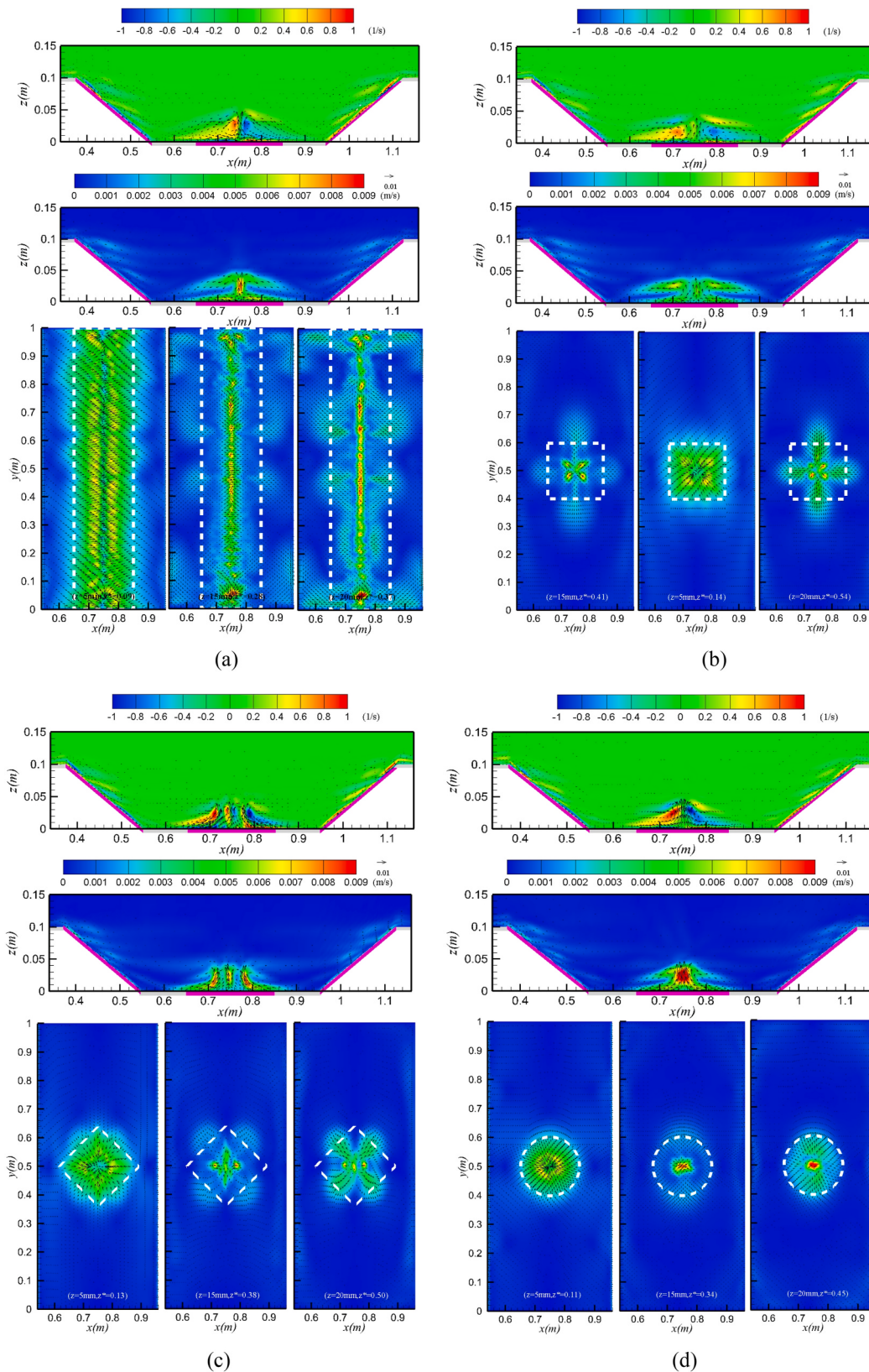


Fig. 10. Velocity fields and vorticity fields under upslope wind effect (a, b, c, and d correspond to cases 5, 6, 7, and 8, which are rectangle, square, rhombus, and circle, respectively).

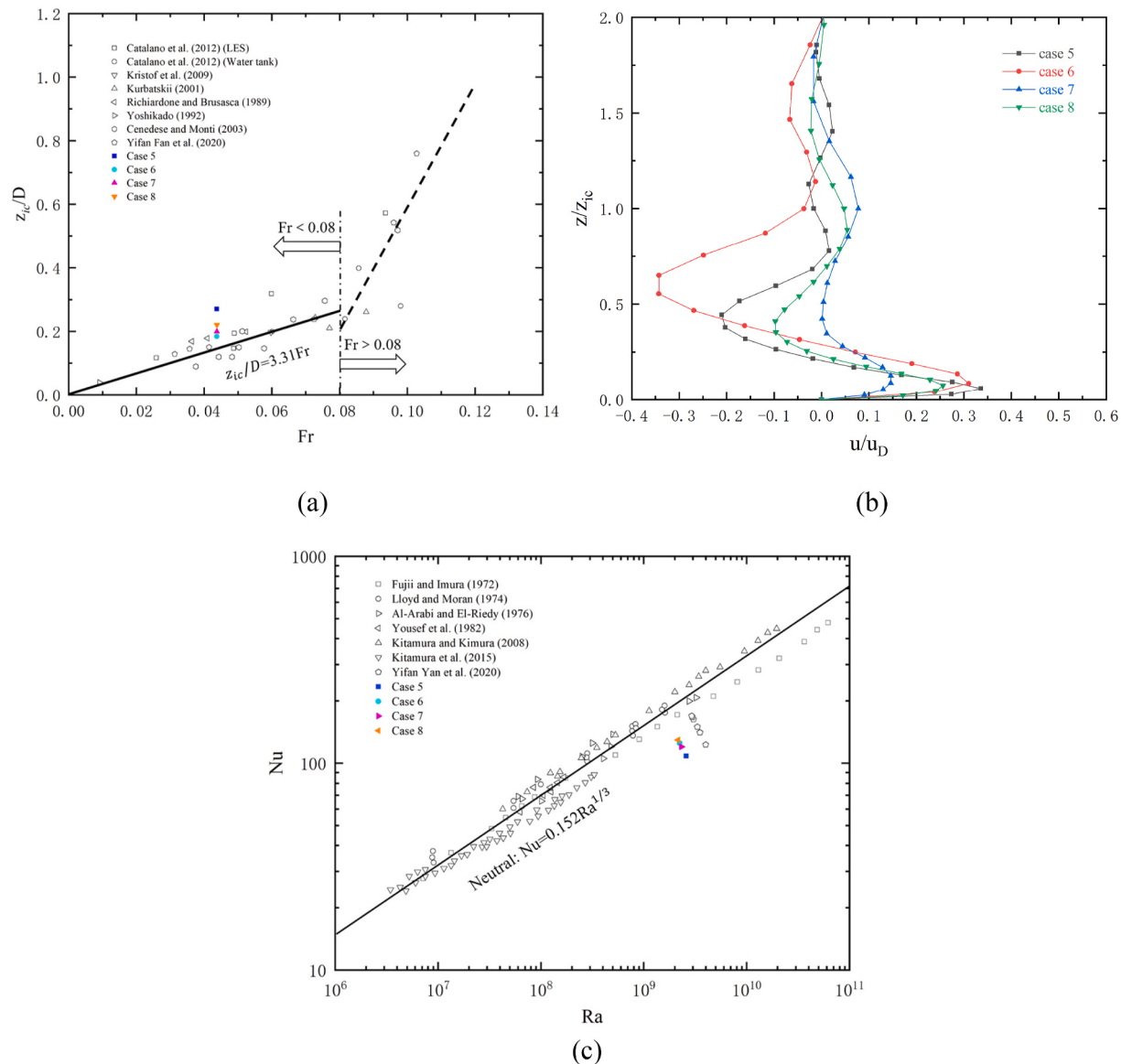


Fig. 11. Under upslope wind effect (cases 5, 6, 7, and 8, which are rectangle, square, rhombus, and circle, respectively); (a) Relationship between Fr and aspect ratio of urban thermal plume; (b) Vertical dimensionless horizontal velocity distribution at urban edges; (c) The relation between Ra and Nu .

the development of the UHIC and is beneficial to the regulation of urban thermal environment, and the “chain flow” phenomenon is formed between the outflow of UHIC and the upslope wind under the action of the upslope wind.

From the perspective of the urban canopy surface heat transfer coefficient, although the heat transfer coefficient will change with the transformation of the urban geometric form, the difference between various forms is not substantial, which needs to be confirmed by numerous detailed research data in the future. The current study ignores the Coriolis force (deflection force of the Earth's rotation) [57], but when the size of the valley city is large, the air will deflate to the right in the Northern Hemisphere (and to the left in the Southern Hemisphere) under the influence of this force, forming a counterclockwise (clockwise) rotation, which changes the characteristics of the mesoscale flow field. In addition, this study is based on the ideal paradigm of a valley city. In the future, it will be necessary to transition the physical model from an ideal model to reality.

5. Conclusions

In this paper, the experimental method of “numerical water tank” was used to study the influences of different valley urban forms on mesoscale flow field characteristics by taking the relative size of the valley floor width to the city diameter and the geometric form of city as the control variables. The flow characteristics and heat transfer coefficient of the urban canopy surface were also evaluated, and the following main conclusions were drawn:

- (1) The existence of valleys restricts the horizontal development of the UHIC and promotes its vertical development to the ground, both from the perspective of the simple terrain effect and the influence of slope wind. Additionally, the existence of the valley promotes the development of the UHIC along the valley axis, and it is most significant under the action of the downslope wind. The temperature difference is the fundamental cause of the UHIC.
- (2) Urban expansion (reduction in R) will lead to the weakening of the urban regional wind speed, but this rule is no longer valid when there is downslope wind action. Furthermore, urban

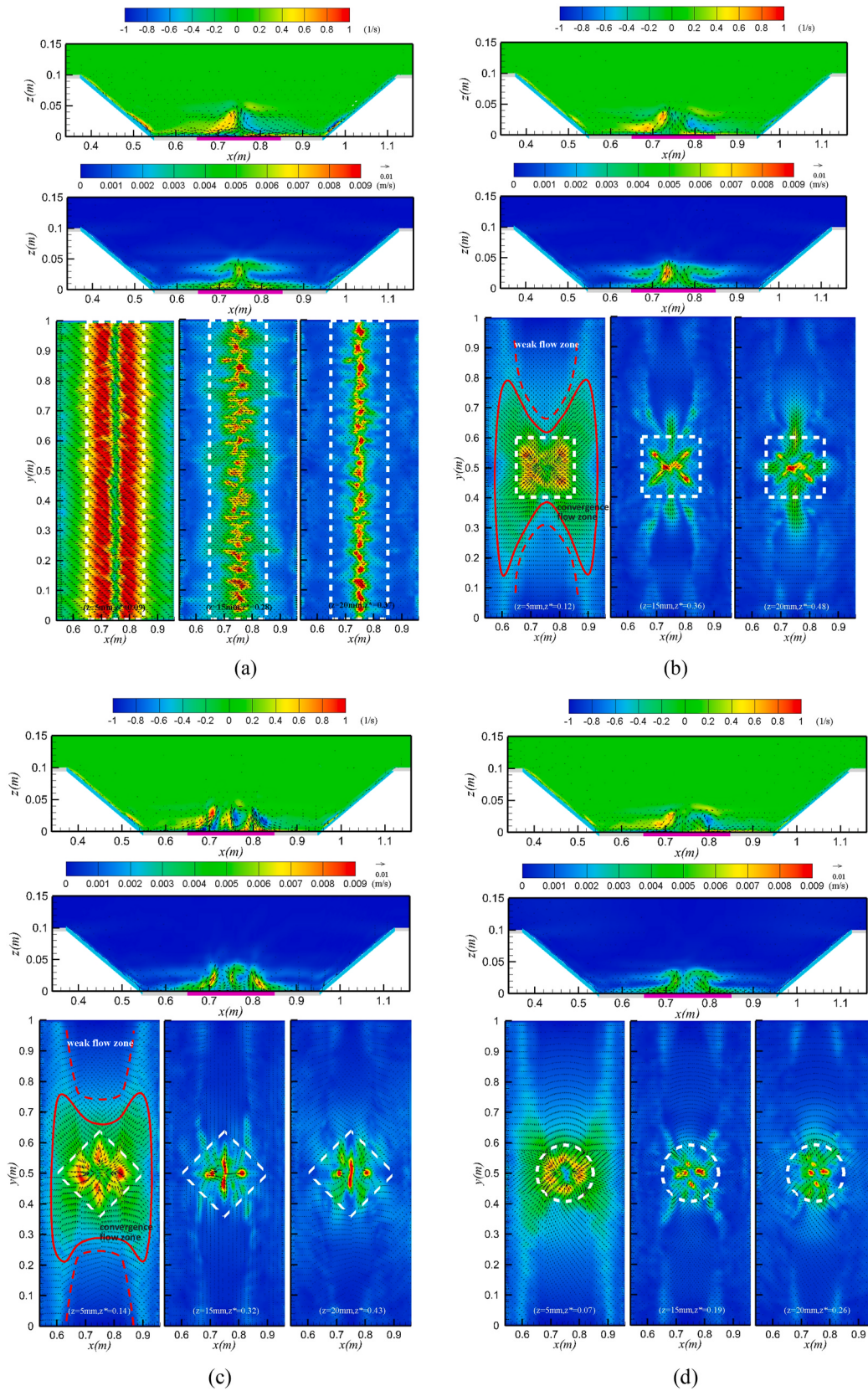


Fig. 12. Velocity fields and vorticity fields under the downslope wind effect (a, b, c, and d correspond to cases 9, 10, 11, and 12, which are rectangle, square, rhombus, and circle, respectively).

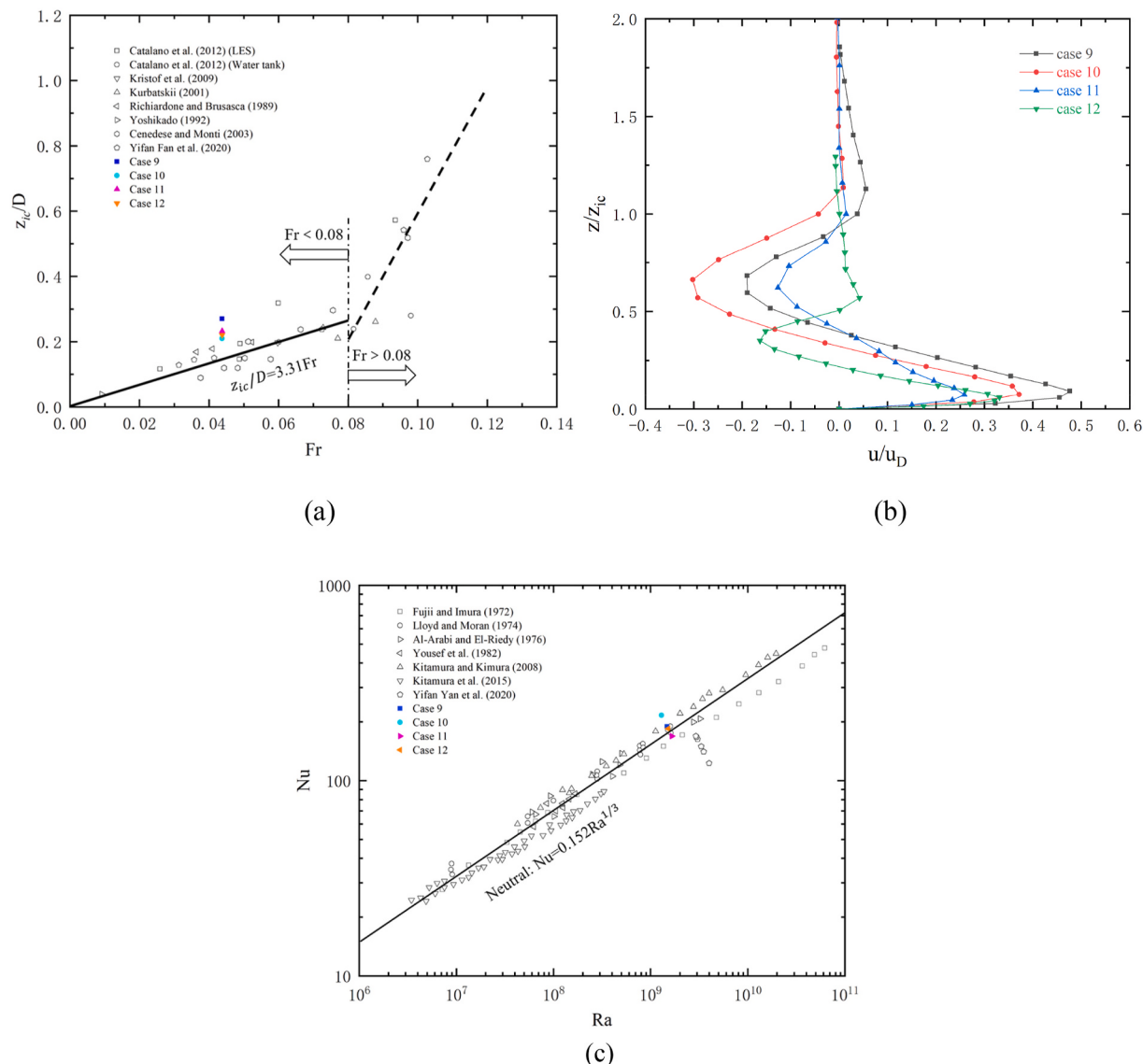


Fig. 13. Under downslope wind effect (cases 9, 10, 11, and 12, which are rectangle, square, rhombus, and circle, respectively) (a) Relationship between Fr and aspect ratio of urban thermal plume; (b) Vertical dimensionless horizontal velocity distribution at urban edges; (c) The relationship between Ra and Nu .

expansion will also lead to a decrease in the urban canopy surface heat transfer coefficient, when the downslope wind action shows the opposite trend. It has been pointed out that if the downslope wind is to be effectively utilized to improve the thermal environment in urban areas, the diameter of the city should reach more than 1/3 of the width of the valley, but the influence of the upslope wind should also be weighed.

- (3) Comparing and analyzing the variations in the mixed height of the city center and the vertical dimensionless horizontal velocity distribution of the four urban layouts of rectangle, square, rhombus, and circle, the atmospheric diffusion conditions of the rectangular and square urban layouts are the most favorable. Two rectangular and square schemes are preferred in the planning of valley cities. In addition, the site selection of the industrial park should fully consider the influence of “diagonal flow” and slope wind, and, in principle, should be far from the diagonal flow area and the convergence flow area formed by the coupling effect of the slope wind and UHIC.
- (4) From the perspective of the urban canopy surface heat transfer coefficient, although the heat transfer coefficient will change with the transformation of the urban geometric form, the

difference between forms is not significant, which needs to be confirmed by substantial detailed research data in the future. The regulation of the urban thermal environment by the downslope wind is more prominent in various urban geometrical conditions.

Declaration of competing interest

The authors declare that they have no known competing financial interests or personal relationships that could have appeared to influence the work reported in this paper.

Acknowledgement

This work was supported by the National Natural Science Foundation of China (No. 52078409) and the National Key Research and Development Program (No. 2018YFC0705300).

References

- [1] T.R. Oke, *The heat island of the urban boundary layer: characteristics, causes and effects*. Wind Climate in Cities, in: NATO ASI Series (Series E: Applied Sciences), vol. 277, Springer, Dordrecht, 1995. D.A.G. Cermak J.E., Plate E.J., Viegas D.X.

- [2] P. Alpert, et al., Global dimming or local dimming?: effect of urbanization on sunlight availability, *Geophys. Res. Lett.* 32 (17) (2005) 317–330.
- [3] Q. Zhao, et al., Study on the influence of fog and haze on solar radiation based on scattering-weakening effect, *Renew. Energy* 134 (APR) (2019) 178–185.
- [4] C. Zhang, et al., An investigation on the attenuation effect of air pollution on regional solar radiation, *Renew. Energy* 161 (2020) 570–578.
- [5] L. Zhang, et al., Seasonal variations of the impact of urban aerosol pollution on distributed solar photovoltaic generation of nine megacities in China, *Urban Climate* 34 (2020) 100723.
- [6] Y. Jiang, et al., Changes in wind speed over China during 1956–2004, *Theor. Appl. Climatol.* 99 (3–4) (2010) 421–430.
- [7] Z. Li, et al., Changes in wind speed and extremes in Beijing during 1960–2008 based on homogenized observations, *Adv. Atmos. Sci.* 28 (2) (2011) 408–420.
- [8] L. Peng, et al., Wind weakening in a dense high-rise city due to over nearly five decades of urbanization, *Build. Environ.* 138 (2018) 207–220.
- [9] Y. Liu, et al., A preliminary study on the influence of Beijing urban spatial morphology on near-surface wind speed, *Urban Climate* 34 (2020) 100703.
- [10] D. Wu, X.J. Wu, F. Li, Temporal and spatial variation of haze during 1951–2005 in Chinese mainland, *Journal of Meteorological Research* 68 (5) (2010) 680–688.
- [11] D. Wu, Hazy weather research in China in the last decade:A review, *Acta Sci. Circumstantiae* 32 (2) (2012) 257–269.
- [12] D. Liu, et al., Urbanization and industrialization effects on haze in China: take Jinagsu for example, *Egu General Assembly Conference*, 2017.
- [13] L. Liang, Z. Wang, J. Li, The effects of urbanization on environmental pollution in rapidly developing urban agglomerations, *J. Clean. Prod.* 237 (2019) 117649.
- [14] X. Yang, Y. Hou, B. Chen, Observed surface warming induced by urbanization in east China, *J. Geophys. Res.: Atmosphere* 116 (2011) D14113.
- [15] K. Jin, et al., Assessment of urban effect on observed warming trends during 1955–2012 over China: a case of 45 cities, *Climatic Change* 132 (4) (2015) 631–643.
- [16] M. Luo, N.C. Lau, Increasing heat stress in urban areas of eastern China: acceleration by urbanization, *Geophys. Res. Lett.* 45 (23) (2018), 13,060–13,069.
- [17] K. Wang, et al., Harmonic analysis of 130-year hourly air temperature in Hong Kong: detecting urban warming from the perspective of annual and daily cycles, *Clim. Dynam.* 51 (1–2) (2018) 613–625.
- [18] G.D. Silcox, et al., Wintertime PM 2.5 concentrations during persistent, multi-day cold-air pools in a mountain valley, *Atmos. Environ.* 46 (2012) 17–24.
- [19] S. Wu, et al., Valley city ventilation under the calm and stable weather conditions: a review, *Build. Environ.* 194 (13) (2021) 107668.
- [20] N. Bei, Typical synoptic situations and their impacts on the wintertime air pollution in the Guanzhong basin, China, *Atmos. Chem. Phys.* 11 (16) (2016) 7373–7387.
- [21] N. Bei, et al., Critical role of meteorological conditions in a persistent haze episode in the Guanzhong basin, China, *Sci. Total Environ.* 550 (2016) 273–284.
- [22] S. Lyman, T. Tran, Inversion structure and winter ozone distribution in the Uintah Basin, *Atmos. Environ.* 123 (2015) 156–165. Utah, USA.
- [23] P.A. Garcia-Chevesich, et al., Respiratory disease and particulate air pollution in Santiago Chile: contribution of erosion particles from fine sediments, *Environ. Pollut.* 187 (2014) 202–205.
- [24] H. Romero, et al., Rapid urban growth, land-use changes and air pollution in Santiago, Chile, *Atmos. Environ.* 33 (24–25) (1999) 4039–4047.
- [25] S. Ye, et al., Characteristics and formation mechanisms of winter haze in Changzhou, a highly polluted industrial city in the Yangtze River Delta, China, *Environ. Pollut.* 253 (Oct) (2019) 377–383.
- [26] H. Li, et al., Typical winter haze pollution in Zibo, an industrial city in China: characteristics, secondary formation, and regional contribution, *Environ. Pollut.* 229 (oct) (2017) 339–349.
- [27] M. Batty, The size, scale, and shape of cities, *Science* 319 (5864) (2008) 769–771.
- [28] A. Schneider, C.E. Woodcock, Compact, dispersed, fragmented, extensive? A comparison of urban growth in twenty-five global cities using remotely sensed data, pattern metrics and census information, *Urban Stud.* 45 (3) (2008) 659–692.
- [29] N. Debbage, J.M. Shepherd, The urban heat island effect and city contiguity, *Comput. Environ. Urban Syst.* 54 (2015) 181–194.
- [30] Z. Wu, D. Li, Principles of Urban planning(In Chinese), China Architecture & Building Press, Beijing, 2010.
- [31] Y. Fan, et al., Conditions for transition from a plume to a dome above a heated horizontal area, *Int. J. Heat Mass Tran.* 156 (2020) 119868.
- [32] Y. Fan, Y. Li, S. Yin, Interaction of multiple urban heat island circulations under idealised settings, *Build. Environ.* 134 (2018) 10–20.
- [33] Y. Fan, et al., Effect of city shape on urban wind patterns and convective heat transfer in calm and stable background conditions, *Build. Environ.* 162 (2019) 106288.
- [34] Y. Fan, Y. Li, Non-uniform ground-level wind patterns in a heat dome over a uniformly heated non-circular city, *Int. J. Heat Mass Tran.* 124 (SEP) (2018) 233–246.
- [35] X. Xu, et al., Characteristics of atmospheric environment of boundary layer structure of city community in BECAPEX and integrate influence, *Acta Meteorol. Sin.* 62 (5) (2004) 663–671.
- [36] Y. Fan, et al., Horizontal extent of the urban heat dome flow, *Sci. Rep.* 7 (1) (2017) 11681.
- [37] Y. Ryu, J.J. Baik, J.Y. Han, Daytime urban breeze circulation and its interaction with convective cells, *Q. J. R. Meteorol. Soc.* 139 (671) (2013) 401–413.
- [38] Gantuya, et al., A numerical study of the interactions of urban breeze circulation with mountain slope winds, *Theor. Appl. Climatol.* 120 (2015) 123–135.
- [39] A. Lemonsu, V. Masson, Simulation of a summer urban breeze over Paris, *Boundary-Layer Meteorol.* 104 (3) (2002) 463–490.
- [40] Z. Bao, A brief introduction of double diffusion convection theory and its research status abroad(In Chinese), *Geol. Sci. Technol. Inf.* (4) (1989) 35–42.
- [41] M. Hibberd, B. Sawford, Design criteria for water tank models of dispersion in the planetary convective boundary layer, *Boundary-Layer Meteorol.* 67 (1–2) (1994) 97–118.
- [42] M. Hibberd, B. Sawford, A saline laboratory model of the planetary convective boundary layer, *Boundary-Layer Meteorol.* 67 (3) (1994) 229–250.
- [43] Y. Abbassi, H. Ahmadike, E. Baniasadi, Prediction of pollution dispersion under urban heat island circulation for different atmospheric stratification, *Build. Environ.* 168 (2019) 106374.
- [44] H. Savijärvi, J. Liya, Local winds in a valley city, *Boundary-Layer Meteorol.* 100 (2) (2001) 301–319.
- [45] G. Huang, N. Tamai, Y.J.D.G.R.B., Kawahara, A numerical investigation of the effect of a slight terrain slope on the urban heat island, *PROCEEDINGS OF HYDRAULIC ENGINEERING* 36 (1992) 507–512.
- [46] G. Ganbat, J.J. Baik, An idealized numerical study of the interactions of urban breeze circulation with mountain slope winds, *11th Symposium on the. 94th American Meteorological Society Meeting, Urban Environment*, 2014.
- [47] X. Wang, Y. Li, Predicting urban heat island circulation using CFD, *Build. Environ.* 99 (2016) 82–97.
- [48] G. Kristóf, N. Rácz, M. Balogh, Adaptation of pressure based CFD solvers for mesoscale Atmospheric problems, *Boundary-Layer Meteorol.* 131 (1) (2009) 85–103.
- [49] Y. Fan, et al., Mean shear flow in recirculating turbulent urban convection and the plume-puff eddy structure below stably stratified inversion layers, *Theor. Appl. Climatol.* 135 (3–4) (2019) 1485–1499.
- [50] L. Shindler, et al., Investigation of local winds in a closed valley: an experimental insight using Lagrangian particle tracking, *J. Wind Eng. Ind. Aerod.* 114 (2013) 1–11.
- [51] M. Moroni, M. Giorgilli, A. Cenedese, Experimental investigation of slope flows via image analysis techniques, *J. Atmos. Sol. Terr. Phys.* 108 (2014) 17–33.
- [52] T. Stathopoulos, Computational wind engineering: Past achievements and future challenges, *J. Wind Eng. Ind. Aerod.* 67–68 (97) (1997) 509–532.
- [53] J. Lu, et al., A laboratory study of the urban heat island in a calm and stably stratified environment. Part I: temperature field, *J. Appl. Meteorol.* 36 (10) (1997) 1377–1391.
- [54] J. Lu, et al., A laboratory study of the urban heat island in a calm and stably stratified environment. Part II: velocity field, *J. Appl. Meteorol.* 36 (10) (1997) 1392–1402.
- [55] W. Wang, The influence of thermally-induced mesoscale circulations on turbulence Statistics over an idealized urban area under a zero background wind, *Boundary-Layer Meteorol.* 131 (3) (2009) 403–423.
- [56] A. Cenedese, P. Monti, Interaction between an inland urban heat island and a sea-breeze flow: a laboratory study, *J. Appl. Meteorol.* 42 (11) (2003) 1569–1583.
- [57] P. Konieczny, T. Yoneda, On dispersive effect of the Coriolis force for the stationary Navier-Stokes equations, *J. Differ. Equ.* 250 (10) (2010) 3859–3873.